Hail climatology for Brisbane, Australia, derived from single-polarization radar and insurance data

Robert Warren*, Hamish Ramsay, Steven Siems, Michael Manton

School of Earth, Atmosphere and Environment, Monash University, Melbourne, Victoria, Australia

Justin Peter, Roger Stone

International Centre for Applied Climate Sciences, University of Southern Queensland, Toowoomba, Queensland, Australia

Alain Protat

Bureau of Meteorology, Melbourne, Victoria, Australia

* Contact: rob.warren@monash.edu

Introduction

- Severe hail storms are a significant hazard along the central east coast of Australia, with previous events causing billions of dollars' worth of damage
- Knowledge of the spatial distribution of these storms is thus relevant both to forecasters and the insurance industry
- Here, the hail hazard in the vicinity of Brisbane (Fig. 1) is quantified using observations from four S-band single-polarization radars and home and contents insurance data provided by Suncorp Group Ltd.

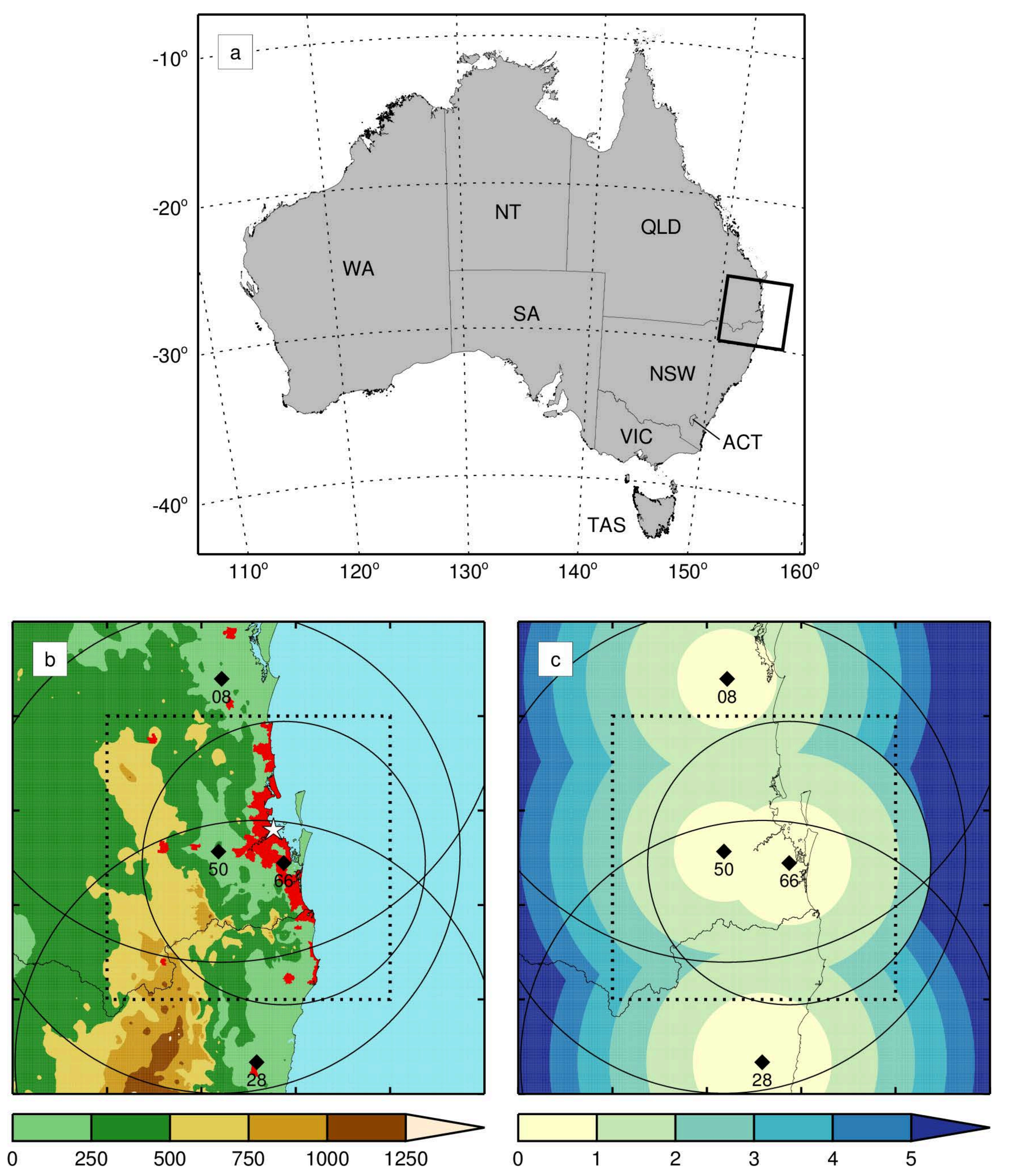

Figure 1. (a) Map of Australia showing the location of the region of interest (black square). (b) Map of region of interest showing topography height (m; colours), location of radars (black diamonds) and their maximum range (black circles), sounding location (white star), regions of high population density (≥100 people km^{-2}; red), and the 300 x 300 km domain used in subsequent analysis (black dotted square). Tick marks on the axes are shown every 100 km. (c) As in (b) but showing the lowest height observable by radar at every point under standard beam propagation (km; colours).

Radar Data

- Archived data from four single-polarization S-band radars (Table 1; Fig. 1) extracted for the period 2008–2015

Table 1. Details of the four S-band radars used in this study. Symbols have the following meaning: ω = angular beam width; $r_{\max}$ = maximum range; Δr = range gate spacing; N_θ = number of elevation sweeps in a volume scan; T = time between volume scans. All radars have an azimuthal beam spacing of 1°, and minimum and maximum elevation angles of 0.5 and 32°, respectively.

ID	Name	Radar	ω (°)	$r_{\max}$ (km)	Δr (m)	N_θ	T (min)
66	Mt Stapylton	Meteor1500S	1.0	150	250	14	6
50	Marburg	WSR74S	1.9	256	1000	15	10
28	Grafton	WSR74S	1.9	256	1000	15	10
08	Gympie	DWSR8502S	2.0	300	500	14	10

- To deal with calibration errors, reflectivity values compared against those from the Ku-band radars on board the Tropical Rainfall Measurement Mission (TRMM) and Global Precipitation Measurement (GPM) satellites
- Volume-matching procedure of Schwaller and Morris (2011) applied with the frequency corrections of Cao et al. (2013)
- Samples filtered to only include those for stratiform precipitation outside the meting layer, at close range (< 100 km), with small time differences (< 3 min), and low reflectivity variance (σ < 8 dB)
- Dates of possible calibration changes identified from radar engineers' activity logs
- Samples between these dates grouped and mean calibration errors quantified using an iterative procedure (Protat et al. 2011)
- Successive periods combined if sample size is too small (< 100) or the difference in calibration error is not statistically significantly based on difference of means test with $p = 95$ %

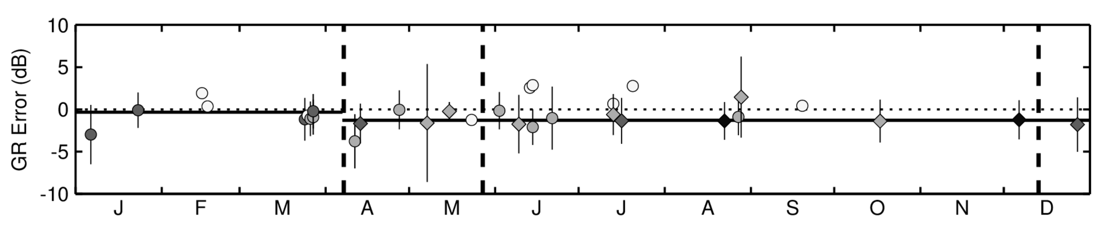

Figure 2. Time series of calibration errors for the Mt Stapylton radar in 2014. Circles and diamonds show the mean error for individual comparisons with TRMM and GPM, respectively, with thin vertical lines denoting the standard deviation. Symbol colours indicate the sample size on a log scale: white = 1–9; light grey = 10–99; dark grey = 100–999; black = 1000+. Thick dashed vertical lines show dates of possible calibration changes and solid horizontal lines show the estimated calibration errors between these dates.

Merging Radars

- Reflectivity data from individual radars merged onto a common three-dimensional grid with 1 km spatial resolution
- Domain is 300 x 300 x 20 km^3, centred just southwest of Brisbane, and includes several major population centres (Fig. 1b), with a total population of around 3.3 million (~15 % of the entire country)
- Minimum radar beam height is < 3 km over almost the entire domain (Fig. 1c) which is below the freezing level during the warm season (~4 km) when virtually all major hail storms occur

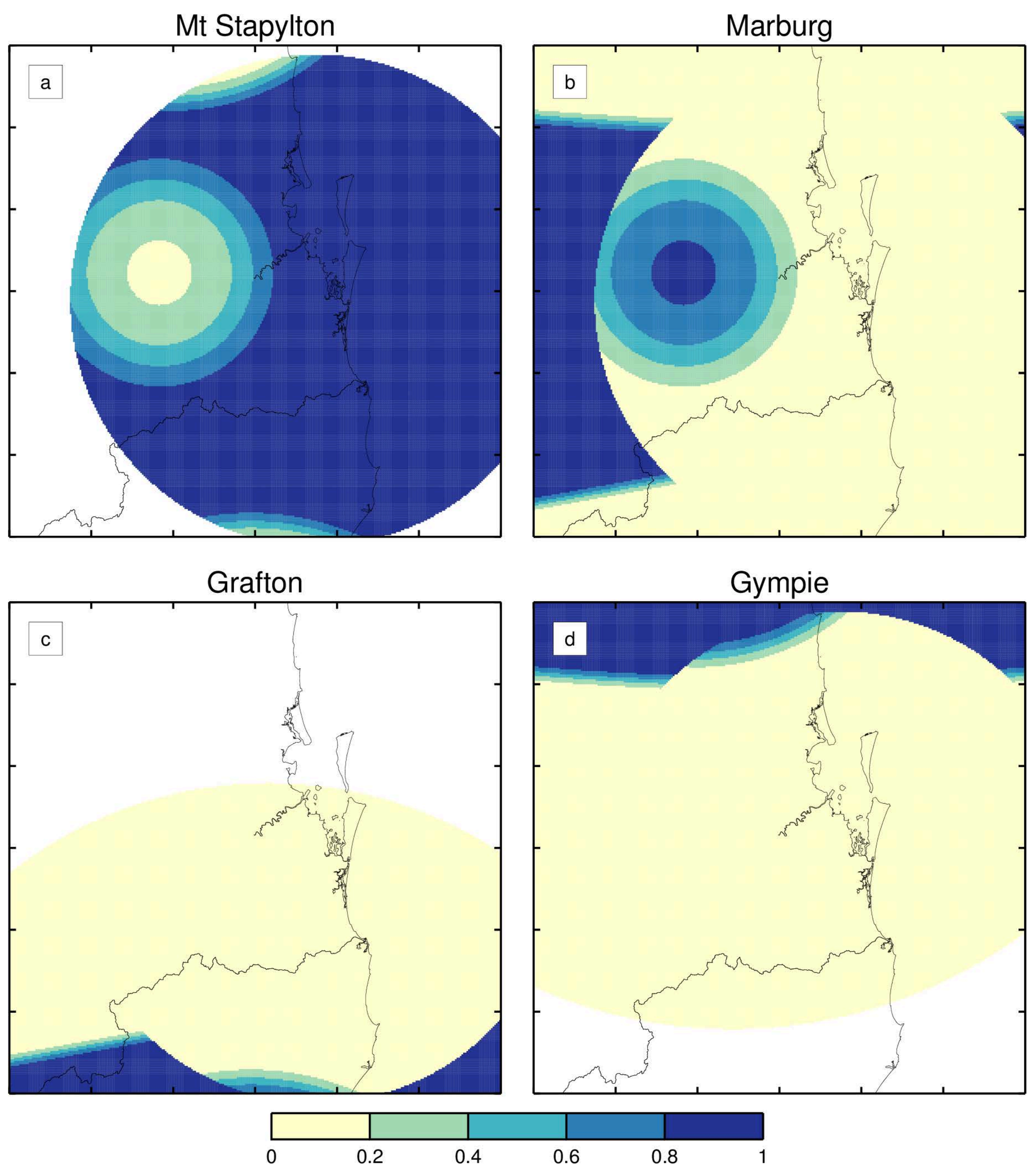

Figure 3. Relative mosaic weights for the four radars. Tick marks on the axes are shown every 50 km.

- Values first averaged in range to a common gate spacing $\Delta r_0 = 1$ km
- Nearest-neighbour mapping applied in range direction and bilinear interpolation applied in azimuth–elevation plane
- Maximum reflectivity value used for oversampled points close to the radar, as recommended by Langston et al. (2007)
- Spatially varying mosaic weights for each radar calculated based on size of radar sample volume relative to grid box size (Fig. 3):

$$w = \exp(-r/r_{\mathrm{scale}})$$

- Here r is the radar range and r_{scale} is the range at which the radar sample volume is equal to the grid box volume $V = 1$ km^3:

$$r_{\mathrm{scale}} = \sqrt{\frac{4V}{\pi\omega^2\Delta r_0}}$$

- Composites produced every 5 min using one scan from each radar either side of the analysis time (±10 min), with linear weighting
- Advection correction applied following Lakshmanan et al. (2006) with domain-wide velocity estimated using cross-correlation

Identifying Damaging Hail

- Home and contents insurance claim and exposure data obtained from Suncorp for a total of 19 days with known hail events
- Using merged radar product and soundings from Brisbane Airport, daily accumulations of the maximum expected size of hail (MESH; Witt et al. 1998) produced for each of these days (e.g. Fig. 4a)
- These were compared against grids showing whether or not damage occurred based on the insurance data (e.g. Fig. 4b) – points with at least three claims [no claims and at least three contracts] were labelled as having damage [no damage]

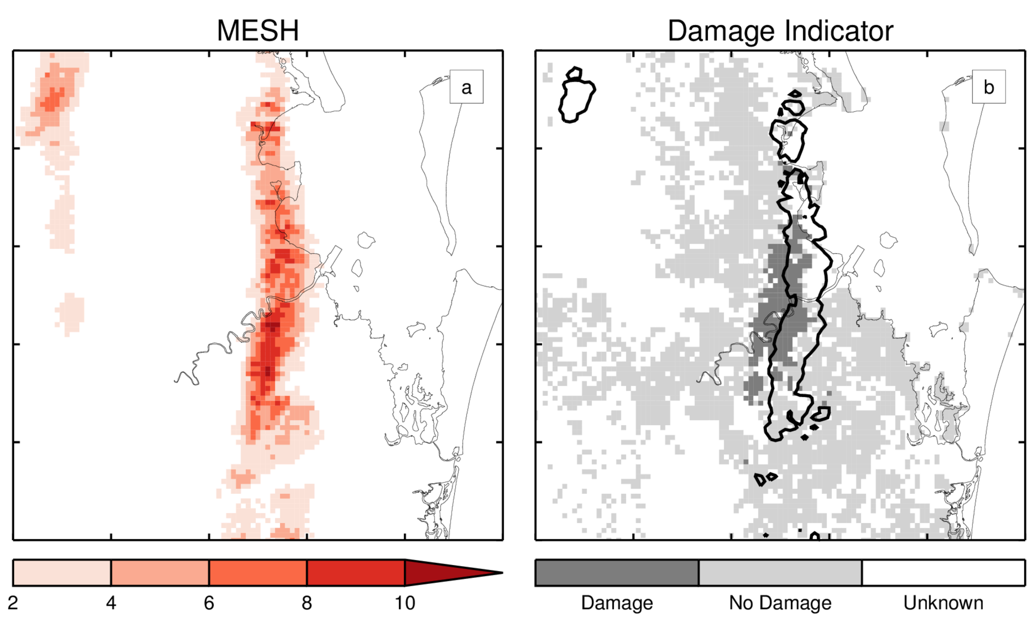

Figure 4. Fields of (a) accumulated MESH (cm) and (b) hail damage for 27/11/2014. The domain shown is 100 x 100 km^2 and approximately centred on Brisbane, with tick marks on the axes shown every 20 km. The MESH = 4.8 cm contour is overlaid in (b) for comparison. There is a pronounced spatial offset in this case, with most of the hail damage located to the west of the high-MESH swath.

- Values extracted for all points with damage/no damage and non-zero MESH values and used to construct 2 x 2 contingency tables for MESH thresholds ranging from 0 to 8 cm in 1 mm increments
- Hit Rate (HR), False Alarm Rate (FAR), and Critical Success Index (CSI) plotted as a function of MESH threshold (Fig. 5)
- CSI peaks at just under 0.2 for MESH = 4.8 cm (with HR = 0.42 and FAR = 0.01); low skill in part reflects spatial offset noted in Fig. 4

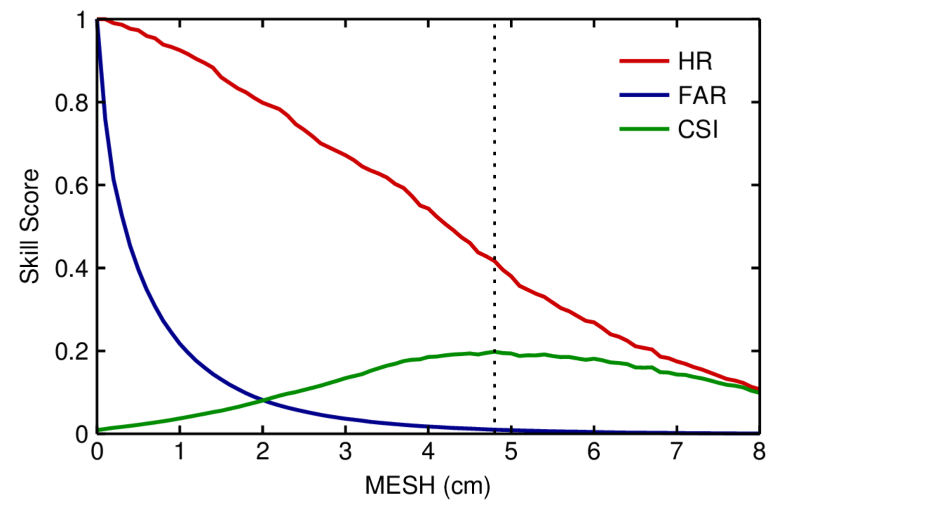

Figure 5. Hit Rate (red), False Alarm Rate (blue), and Critical Success Index (green) plotted as a function of MESH. Vertical dotted line indicates the MESH value corresponding to the maximum CSI.

Hail Climatology

- 617 storm days identified for seven-year period 07/2008–06/2015 based on strike counts from the Global Position and Tracking Systems (GPATS) lightning detection network (Fig. 6)
- Of these, 220 rejected due to missing radar scans (most in the first 12 months), leaving 397 to analyse

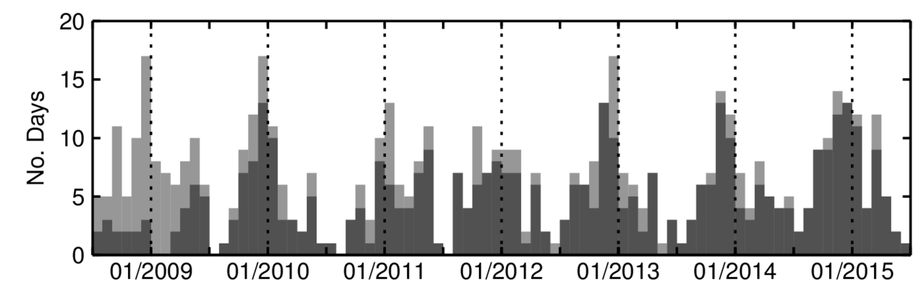

Figure 6. Time series of monthly count of all storm days (light grey) and those with radar data (dark grey).

- MESH accumulations produced for all days and used to derive two products: damaging hail count and maximum MESH (Fig. 7)
- There appears to be a hotspot for large, damaging hail just to the southwest of Brisbane
- This feature was also noted by Soderholm et al. (2016) in their longer (18-year) single-radar (Marburg) climatology
- Hotspot is hypothesised to be caused by favourable interactions between orographically triggered storms and the sea breeze

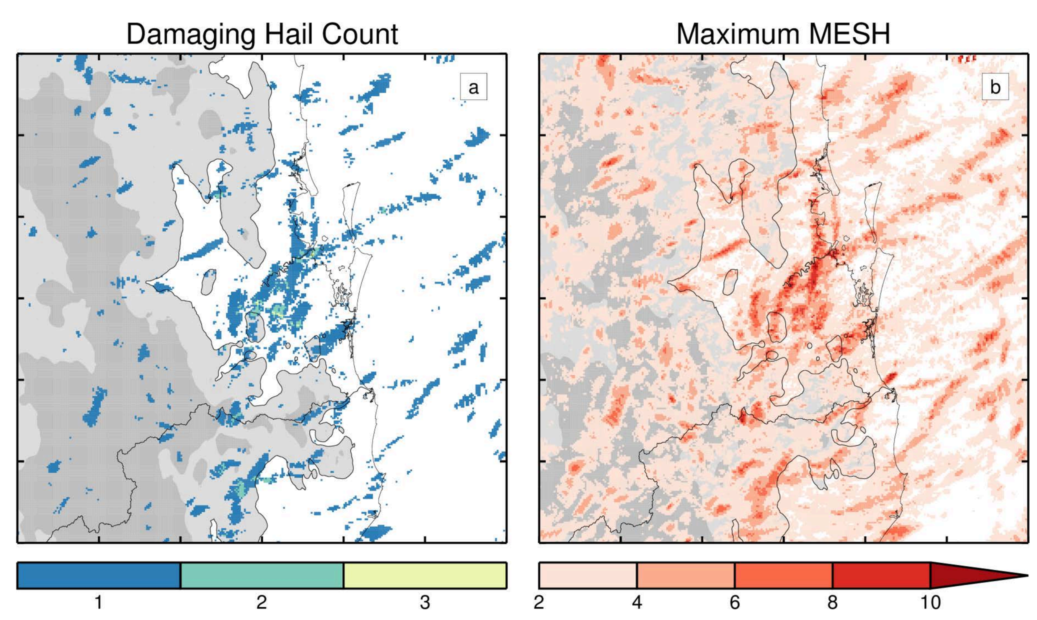

Figure 7. Fields of (a) damaging hail count and (b) maximum MESH (cm) for the seven-year period 07/2008–06/2015. The former was derived using the optimal MESH threshold of 4.8 cm. Topography over 250 m [500 m] is shaded light [dark] grey and the 250 m topography contour is shown. Tick marks on the axes are shown every 50 km.

Future Work

- Explore methods for improving skill of MESH (e.g. tilted integrations, optimal shift, dilation)
- Examine seasonal and diurnal variations in hail occurrence
- Examine large-scale and local environments characterising hail days
- Use high-resolution numerical simulations to explore interactions between convective storms and the sea breeze in Southeast QLD
- Repeat analysis for Sydney region

References

Cao Q, Hong Y, Qi Y, Wen Y, Zhang J, Gourley JJ, Liao L. Empirical conversion of the vertical profile of reflectivity from Ku-band to S-band frequency. *J. Geophys. Res.*, **118**: 1814–1825.

Lakshmanan V, Smith T, Hondl K, Stumpf GJ, Witt A. 2006. A real-time, three-dimensional, rapidly updating, heterogeneous radar merger technique for reflectivity, velocity, and derived products. *Wea. Forecasting*, **21**: 802–823.

Langston C, Zhang J, Howard K. 2007. Four-dimensional dynamic radar mosaic. *J. Atmos. Oceanic Technol.*, **24**: 776–790.

Protat A, Bouniol D, O'Conner EJ, Klein Baltink H, Verlinde J, Widener K. 2011. Cloudsat as a global radar calibrator. *J. Atmos. Oceanic Technol.*, **28**: 445–452.

Schwaller MR, Morris KR. 2011. A ground validation for the Global Precipitation Measurement mission. *J. Atmos. Oceanic Technol.*, **28**:301–319.

Soderholm J, McGowan H, Richter H, Walsh K, Weckwerth T, Coleman M. 2016. The Coastal Convective Interactions Experiment (CCIE): Understanding the role of sea breezes for hailstorm hotspots in Eastern Australia. *Bull. Amer. Meteor. Soc.*, **97**: 1687–1698.

Witt A, Eilts MD, Stumpf GJ, Johnson JT, Micthell ED, Thomas KW. 1998. An enhanced hail detection algorithm for the WSR-88D. *Wea. Forecasting*, **13**: 286–303.